DMD Fast Forward. Published on October 22, 2018 as DOI: 10.1124/dmd.118.083832
This article has not been copyedited and formatted. The final version may differ from this version.

TITLE PAGE

Mechanistic in vitro studies indicate that the clinical drug-drug interaction between telithromycin and simvastatin acid is driven by time-dependent inhibition of CYP3A4 with minimal effect on OATP1B1

ROBERT ELSBY, VICTORIA HARE, HANNAH NEAL, SAMUEL OUTTERIDGE, CATHERINE PEARSON, KATIE PLANT, RACHEL UPCOTT GILL, PHILIP BUTLER, AND ROBERT J RILEY

Department of ADME Sciences, Cyprotex Discovery Ltd (an Evotec company), No 24 Mereside, Alderley Park, Macclesfield, Cheshire, United Kingdom (RE, VH, HN, SO, CP, KP, RUG, PB), Drug Metabolism and Pharmacokinetics, Evotec, Abingdon, Oxfordshire, United Kingdom (RJR).

Downloaded from dmd.aspetjournals.org at ASPET Journals on November 15, 2019

DMD Fast Forward. Published on October 22, 2018 as DOI: 10.1124/dmd.118.083832
This article has not been copyedited and formatted. The final version may differ from this version.

RUNNING TITLE PAGE

Running title: Time-dependent inhibition of CYP3A4 by telithromycin

Corresponding author:

Dr. Robert Elsby

Head of Drug Transporter Sciences,

Cyprotex Discovery Limited,

No 24 Mereside,

Alderley Park,

Cheshire

SK10 4TG

United Kingdom

Tel: +44 (0)1625 505181

Email: r.elsby@cyprotex.com

Number of text pages = 32

Number of tables = 4

Number of figures = 3

Number of references = 26

Number of words in Abstract = 242

Number of words in Introduction = 743

Number of words in Discussion = 1466

Non-standard abbreviations:

AICc, Akaike's Information Criterion; AUC, area under the plasma concentration–time curve; AUCR, area under the plasma concentration–time curve ratio; C_{max}, maximum plasma concentration; CYP, cytochrome P450; DDI, drug-drug interaction; DMSO; dimethyl sulfoxide; f_e, fraction excreted value; f_m, fraction metabolised value; IC_{50}, concentration that

Downloaded from dmd.aspetjournals.org at ASPET Journals on November 15, 2019

DMD Fast Forward. Published on October 22, 2018 as DOI: 10.1124/dmd.118.083832
This article has not been copyedited and formatted. The final version may differ from this version.

produces 50% inhibition; k_{deg}, apparent first-order degradation constant of enzyme; K_i, absolute inhibition constant; K_I, inhibitor concentration that causes half-maximal inactivation of enzyme; k_{inact}, maximal rate of inactivation of enzyme; K_m, Michaelis-Menten kinetic constant; k_{obs}, inactivation rate constant; OATP, organic anion transporting polypeptide.

Downloaded from dmd.aspetjournals.org at ASPET Journals on November 15, 2019

DMD Fast Forward. Published on October 22, 2018 as DOI: 10.1124/dmd.118.083832
This article has not been copyedited and formatted. The final version may differ from this version.

ABSTRACT

A previous attempt to accurately quantify the increased simvastatin acid exposure due to drug-drug interaction (DDI) with coadministered telithromycin, using a mechanistic static model, substantially underpredicted the magnitude of area under the plasma concentration-time curve ratio (AUCR) based on reversible inhibition of cytochrome P450 (CYP) 3A4 and organic anion transporting polypeptide (OATP) 1B1 (Elsby et al., 2012). In order to reconcile this disconnect between predicted and clinically observed AUCR, telithromycin was evaluated as a time-dependent inhibitor of CYP3A4 in vitro, as well as an inhibitor of OATP1B1. Telithromycin inhibited OATP1B1-mediated [^{3}H]-estradiol 17β-D-glucuronide (0.02 μM) transport with a mean IC_{50} of 12.0±1.45 μM and was determined by IC_{50} shift and kinetic analyses to be a competitive reversible inhibitor of CYP3A4-mediated midazolam 1-hydroxylation with a mean K_i of 3.65±0.531 μM. The 2.83-fold shift in IC_{50} (10.4 μM to 3.68 μM) following a 30-min metabolic pre-incubation confirmed telithromycin as a time-dependent inhibitor of CYP3A4; determined mean K_I and k_{inact} values for inactivation being 1.05±0.226 μM and 0.02772±0.00272 min^{-1}, respectively. Following integration of an enzyme time-dependent inhibition component into the previous mechanistic static model using the in vitro inhibitory kinetic parameters determined above, the newly predicted simvastatin acid AUCR (10.8 or 5.4) resulting from perturbation of its critical disposition pathways matched the clinically observed AUCR (10.8 or 4.3) following co-administration, or staggered administration, with telithromycin, respectively. These results indicate time-dependent inhibition of CYP3A4 by telithromycin as the primary driver underlying its clinical DDI with simvastatin acid.

Downloaded from dmd.aspetjournals.org at ASPET Journals on November 15, 2019

DMD Fast Forward. Published on October 22, 2018 as DOI: 10.1124/dmd.118.083832
This article has not been copyedited and formatted. The final version may differ from this version.

INTRODUCTION

Simvastatin acid, administered as inactive lactone simvastatin at an oral dose of 5-80 mg/day, is a 3-hydroxy-3-methylglutaryl (HMG)-coenzyme-A reductase inhibitor (statin) that was developed to treat hypercholesterolemia (Zocor® label). The critical disposition pathways of simvastatin acid, following its formation from the lactone in the intestinal wall, and their contributions to overall clearance (fraction metabolised or excreted values; f_m or f_e) have been determined previously based on derivation from clinical human mass balance, pharmacogenetic and drug-drug interaction (DDI) evidence (Elsby et al., 2012). These pathways include intestinal cytochrome P450 3A4 (CYP3A4, f_m = 0.4) as the barrier to simvastatin acid absorption, and the hepatic uptake transporter organic anion transporting polypeptide 1B1 (OATP1B1, f_e = 0.79) and hepatic CYP3A4 (f_m = 0.83) which are responsible for hepatic elimination of simvastatin acid (Elsby et al., 2012).

Drug-drug interactions with simvastatin acid are of clinical concern as elevated systemic concentrations of statins, due to perturbation of critical disposition pathways, are associated with increased muscle exposure and risk of myopathy or even fatal rhabdomyolysis in extreme cases (Egan and Colman, 2011). Indeed, clinically significant DDIs (resulting in up to 10-fold increases in simvastatin acid exposure; defined as area under the plasma concentration-time curve, AUC) have been observed between simvastatin acid and CYP3A4 inhibitors such as telithromycin and clarithromycin (Zocor® drug label, Ketek® drug label). Furthermore, DDIs can also result from inhibition of OATP1B1 either alone (e.g. with gemfibrozil; simvastatin acid AUC ratio (AUCR) = 2.85), or in combination with inhibition of CYP3A4 (e.g. with cyclosporine; simvastatin acid AUCR = 8.0) (Elsby et al., 2012).

Understanding the potential for a new investigational drug to perpetrate DDIs with co-administered medications in the clinic is an important part of the drug discovery and

Downloaded from dmd.aspetjournals.org at ASPET Journals on November 15, 2019

DMD Fast Forward. Published on October 22, 2018 as DOI: 10.1124/dmd.118.083832
This article has not been copyedited and formatted. The final version may differ from this version.

development process. Such analysis involves initial in vitro evaluation of the drug as an inhibitor of individual enzymes/transporters to determine a K_i, which is then put into context with anticipated concentration at the interaction site using basic static equations detailed in regulatory guidance (FDA draft DDI guidance 2017). However, the industry is moving towards adopting mechanistic static model approaches that allow calculation of theoretical AUCR changes for victim drugs due to inhibition of multiple critical disposition pathways in order to enable more effective, quantitative, predictions of increasingly complex DDIs (Williamson and Riley, 2017). Such predictions can be used during drug discovery or development to inform either decision-making or clinical protocol design for patient studies, respectively (Williamson and Riley, 2017).

One such published mechanistic static model described the prediction of AUCRs for twenty clinically observed DDIs with six statin drugs following inhibition of one or more drug (victim)-specific critical disposition pathways (Elsby et al., 2012). This model successfully predicted 90% of DDIs within two-fold of the clinically observed AUCR (Williamson and Riley, 2017). Interestingly, one of the two DDIs that did not predict in the model was the interaction between simvastatin acid and telithromycin which underpredicted the observed DDI almost three-fold (predicted AUCR = 4.0), based upon composite inhibition of intestinal CYP3A4 (predicted 1.67-fold AUC increase), hepatic OATP1B1 (predicted 1.2-fold AUC increase) and hepatic CYP3A4 (predicted 2.0-fold AUC increase). The authors hypothesised that this underprediction of AUCR could be due to telithromycin being a possible time-dependent inhibitor of CYP3A4 in vivo based on the findings of a sponsor-conducted clinical trial demonstrating a reduced (compared to co-administration) but clinically significant DDI between the drugs even when they are administered 12 hours apart. If this was indeed the case, then the Rowland-Matin equation used in the model would be expected to underestimate AUCR as it only considers reversible CYP inhibition (Elsby et al.,

Downloaded from dmd.aspetjournals.org at ASPET Journals on November 15, 2019

DMD Fast Forward. Published on October 22, 2018 as DOI: 10.1124/dmd.118.083832
This article has not been copyedited and formatted. The final version may differ from this version.

2012). However, whilst a recent report utilised an in silico model to estimate time-dependent inhibitory parameters for telithromycin towards verifying such a mechanism (Vieira et al., 2012), as far as these authors can observe from searching the literature, to date no study appears to have been reported that has confirmed whether telithromycin is a time-dependent inhibitor of CYP3A4 in vitro.

Therefore, the aims of this study were to investigate telithromycin as both a reversible and time-dependent inhibitor of CYP3A4 in pooled human liver microsomes and to utilise the in vitro determined enzyme inhibitory kinetic parameters, alongside that determined against OATP1B1. Using these data in a modified version of the mechanistic static statin model described by Elsby et al. (2012), now integrating a time-dependent (inactivation) component for enzyme (CYP3A4), an attempt was made to reconcile the disconnect between predicted and observed AUCR for the clinical DDI with simvastatin acid.

Downloaded from dmd.aspetjournals.org at ASPET Journals on November 15, 2019

DMD Fast Forward. Published on October 22, 2018 as DOI: 10.1124/dmd.118.083832
This article has not been copyedited and formatted. The final version may differ from this version.

MATERIALS AND METHODS

Materials

Estradiol 17β-D-glucuronide, ketoconazole, metoprolol, mifepristone, rifamycin SV, midazolam, NADPH, sodium butyrate, non-essential amino acids and HEPES were purchased from Sigma-Aldrich (Poole, Dorset, UK). Telithromycin was purchased from Toronto Research Chemicals (Ontario, Canada). Midazolam was purchased from Tocris (Oxfordshire, UK). [^{3}H]-Estradiol 17β-D-glucuronide and Optiphase Supermix liquid scintillation cocktail and 24-well liquid scintillation counting visiplates were purchased from PerkinElmer Life and Analytical Sciences (Buckinghamshire, UK). Hanks balanced salt solution (Gibco™ HBSS; containing $CaCl_2$ and $MgCl_2$), Dulbecco's modified eagle medium (Gibco™ DMEM; high glucose with GlutaMax and pyruvate), fetal bovine serum (Gibco™; heat inactivated) and mammalian protein extraction reagent (M-PER) were purchased from Fisher Scientific (Loughborough, UK). All other chemicals, solvents and reagents were purchased from Fisher Scientific.

Biocoat™ Poly-D-lysine 24-well multiwell plates, human organic anion transporting polypeptide (OATP) 1B1 (SLCO1B1)-expressing TransportoCells™ and vector control cells, and pooled human liver microsomes were supplied by Corning BV Life Sciences (Amsterdam, The Netherlands). 96-Well deep well Abgene polypropylene plates, 96-well v-bottom polypropylene plates, 96-well deep well 1 mL polypropylene plates or 96-well shallow round-bottomed polypropylene plates were supplied by Fisher Scientific.

Assessment of telithromycin as an inhibitor of OATP1B1

OATP1B1 and vector control cell lines were seeded in cell culture medium (consisting of Dulbecco's modified eagles medium supplemented with 10% (w/v) fetal bovine serum and 1% (v/v) nonessential amino acids) at 3-4 x 10^5 cells per well in 24-well poly-D-lysine coated

Downloaded from dmd.aspetjournals.org at ASPET Journals on November 15, 2019

DMD Fast Forward. Published on October 22, 2018 as DOI: 10.1124/dmd.118.083832
This article has not been copyedited and formatted. The final version may differ from this version.

plates to achieve a pre-assay confluence of typically 80 – 95%. The media was changed 3-4 h post-seeding and the cells were cultured in media containing 2 mM sodium butyrate at 37 °C, 8% CO_2 for 24 h. Prior to the assay, cells were washed twice with pre-warmed uptake buffer (HBSS containing 10 mM HEPES, pH 7.4) then left to pre-incubate with telithromycin (0.3, 1, 3, 10, 30 or 100 µM) in warm uptake buffer for 15 min. After the pre-incubation, uptake buffer was removed and the appropriate incubation solutions were added to the wells.

Uptake of the probe substrate [^{3}H]-estradiol 17β-D-glucuronide (0.02 µM) was determined (in triplicate wells per condition, on three separate occasions) over a 2 min incubation time at 37 °C in OATP1B1-expressing cells and vector control cells, in the absence and presence of telithromycin (0.3, 1, 3, 10, 30 or 100 µM) or the positive control inhibitor rifamycin SV (100 µM), at a final dimethyl sulfoxide (DMSO) concentration of 1% (v/v). At the end of the incubation, active transport processes were terminated by removing (via aspiration) the incubation solutions, immediately washing the cells twice with ice cold uptake buffer and then placing plates on ice. Following the wash steps, M-PER (400 µL) was added to each well and cells were lysed for at least 5 min at 250 rpm on an orbital shaker. An aliquot (300 µL) of cell lysate was added to a white walled, clear bottomed 24-well visiplate, liquid scintillation cocktail (2 mL) was added, and samples were counted on a Microbeta2 scintillation counter (PerkinElmer) in order to determine the total radioactivity (dpm) taken up in cells. Separately, the protein content of cell lysates (25 µL) was determined using a Bicinchoninic acid (BCA) protein assay kit according to the manufacturer's instructions.

For data analysis, the determined total uptake of probe substrate [^{3}H]-estradiol 17β-D-glucuronide into cells (pmol) was normalised to the protein (mg) content of each well to calculate the uptake activity (pmol/mg). Uptake activity of probe substrate into transporter-expressing cells was corrected for that determined into vector control cells to calculate the transporter-mediated (corrected) uptake. Corrected uptake activity (pmol/mg)

Downloaded from dmd.aspetjournals.org at ASPET Journals on November 15, 2019

DMD Fast Forward. Published on October 22, 2018 as DOI: 10.1124/dmd.118.083832
This article has not been copyedited and formatted. The final version may differ from this version.

was converted to percentage (vehicle) control activity, which was subsequently plotted against nominal inhibitor concentration and fitted using SigmaPlot 12.5 (Systat Software Inc., Chicago, IL; four parameter logistic equation) to determine the concentration that produces half-maximal inhibition of probe substrate transport (IC_{50}; equivalent to K_i as probe substrate concentration in the assay is at least 10-times lower than its K_m, and assuming competitive inhibition).

Assessment of telithromycin as a reversible or time-dependent inhibitor of CYP3A4 by IC_{50} shift assay

Six concentrations of telithromycin (0.4, 1, 4, 10, 40 and 100 µM; final DMSO concentration 0.25% v/v) and pooled human liver microsomes (final concentration 0.1 mg/mL) were either pre-incubated at 37 °C in 0.1 M phosphate buffer (pH 7.4) for 30 min in the absence and presence of NADPH (1 mM), or underwent no pre-incubation (termed zero minute pre-incubation). At the end of the pre-incubation period, the CYP3A4 probe substrate midazolam (2.5 µM; equivalent to K_m) and NADPH (1 mM) were then added (final DMSO concentration 0.26% v/v) and the samples incubated for 5 min at 37 °C. The time-dependent inhibitor, mifepristone (0.2, 0.5, 2, 5, 20 and 50 µM), was incubated alongside telithromycin as a positive control. Incubations were performed in singlicate wells per condition.

Following the incubation period, reactions were terminated by the addition of two-volumes of ice-cold methanol and subsequently centrifuged at 1400 g for 30 min at 4 °C to remove precipitated protein. An aliquot (40 µL) of each supernatant was transferred to a 96-well Abgene plate containing 0.1% (v/v) aqueous formic acid and internal standard (metoprolol) solution (60 µL). Formation of the metabolite 1-hydroxymidazolam was monitored by peak area response (using metoprolol as internal standard) by liquid chromatography-tandem mass spectrometry in positive-ion mode using a parent to daughter transition of 342.108 to 203.045 as described below. Metabolite peak area response in the

Downloaded from dmd.aspetjournals.org at ASPET Journals on November 15, 2019

DMD Fast Forward. Published on October 22, 2018 as DOI: 10.1124/dmd.118.083832
This article has not been copyedited and formatted. The final version may differ from this version.

presence of telithromycin was converted to percentage (vehicle) control activity, which was subsequently plotted against nominal inhibitor concentration and fitted using WinNonLin (model 103 with Levenburg-Marquardt algorithm) to determine the concentration that produces half-maximal inhibition of probe substrate metabolism (IC_{50}).

Assessment of telithromycin as a reversible inhibitor of CYP3A4 (K_i determination)

Six concentrations of telithromycin (1, 2.5, 5, 10, 25 and 50 µM; equivalent to approximately 0.1xIC_{50}, 0.25xIC_{50}, 0.5xIC_{50}, 1xIC_{50}, 2.5xIC_{50} and 5xIC_{50}) were pre-incubated for 5 min at 37 °C in 0.1 M phosphate buffer (pH 7.4) containing pooled human liver microsomes (final concentration 0.1 mg/mL) and the CYP3A4 probe substrate midazolam at five different concentrations (0.75, 2.5, 5, 10 and 15 µM; equivalent to approximately 0.3xK_m, 1xK_m, 2xK_m, 4xK_m and 6xK_m). Following the pre-incubation period, reactions were initiated by the addition of NADPH (1 mM) and incubated for 30 min (final DMSO concentration 0.3% v/v). A vehicle control incubation containing DMSO instead of telithromycin was included with each substrate concentration, and a positive control inhibitor ketoconazole (0.008, 0.02, 0.04, 0.06, 0.08 and 0.2 µM; equivalent to approximately 0.1xIC_{50}, 0.25xIC_{50}, 0.5xIC_{50}, 0.75xIC_{50}, 1xIC_{50} and 2.5xIC_{50}) was incubated alongside. Incubations were performed in duplicate wells per condition on three separate occasions.

Following the incubation period, reactions were terminated, processed and analysed for the metabolite 1-hydroxymidazolam as described above (IC_{50} shift). Regression analysis of enzyme kinetic data (based on metabolite peak area response) was carried out using the Enzyme Kinetics module of SigmaPlot 12.5, using models for competitive, non-competitive, uncompetitive and mixed inhibition according to the equations displayed in Table 1. The K_i value of telithromycin was determined using each inhibition type model. The goodness of fit criteria used to select the most appropriate inhibition model comprised of visual inspection of

Downloaded from dmd.aspetjournals.org at ASPET Journals on November 15, 2019

DMD Fast Forward. Published on October 22, 2018 as DOI: 10.1124/dmd.118.083832
This article has not been copyedited and formatted. The final version may differ from this version.

the data (Michaelis-Menten, Eadie-Hofstee and Lineweaver-Burk plots), squared correlation coefficient (R^2) and corrected Akaike's Information Criterion (AICc).

Inactivation of CYP3A4 by telithromycin (K_I and k_{inact} determinations)

The concentration range of inhibitor, pre-incubation times and dilution factor were determined from the reversible inhibition and time dependent inhibition assays conducted above. Seven concentrations of telithromycin (0.4, 0.8, 2, 4, 8, 20 and 40 µM), or the positive control mifepristone (0.2, 0.4, 1, 2, 4, 10 and 20 µM), plus a vehicle control (0.25% v/v DMSO in pre-incubation) were pre-incubated in 0.1 M phosphate buffer (pH 7.4) at 37 °C containing human liver microsomes (0.1 mg/mL) and NADPH (1 mM) for a range of five pre-incubation times, (5, 10, 15, 20 and 30 min) plus a 0 min pre-incubation, in duplicate wells and on three separate occasions. At the end of the individual pre-incubations, an aliquot of the pre-incubation mixture was added to an incubation mixture, in a 1:10 dilution, with the specific CYP3A4 probe substrate, midazolam (12.5 µM, equivalent to 5xK_m) and NADPH (1 mM) for a 5 min incubation at 37 °C (final DMSO of 0.075% v/v and final microsomal concentration of 0.01 mg/mL). This procedure diluted telithromycin to one tenth of its original concentration in order to reduce any impact of reversible inhibition on CYP3A4. Following the incubation period, reactions were terminated, processed and analysed for the metabolite 1-hydroxymidazolam as described above (IC_{50} shift).

The decrease in the formation of the metabolite compared to the vehicle control at each pre-incubation time was used to calculate k_{inact} and K_I. Briefly, the average activity remaining was determined at each telithromycin/mifepristone concentration as a percent of the vehicle control activity for the specific pre-incubation time in order to account for any loss of metabolic activity over time. The natural logarithm of the corrected percent remaining activity was then plotted versus pre-incubation time for each inhibitor concentration and linear least squares regression enabled the k_{obs} (observed initial rate of

Downloaded from dmd.aspetjournals.org at ASPET Journals on November 15, 2019

DMD Fast Forward. Published on October 22, 2018 as DOI: 10.1124/dmd.118.083832
This article has not been copyedited and formatted. The final version may differ from this version.

inactivation for each inhibitor concentration) to be calculated. Non-linear regression analysis of the k_{obs} data versus pre-incubation inhibitor concentration was performed using the Enzyme Kinetics module of SigmaPlot 12.5 in order to determine k_{inact} and K_I values from the modified Michaelis-Menten equation:

$$k_{obs} = \frac{k_{inact} \cdot [I]}{(K_I + [I])}$$

where k_{obs} is the inactivation rate constant, k_{inact} is the maximal rate of inactivation (analogous to V_{max}), [I] is the inhibitor concentration and K_I is the inhibitor concentration that causes half the maximal rate of inactivation (analogous to K_m).

Liquid Chromatography-Mass Spectrometry

The system consisted of an Acquity™ Binary Solvent Manager (BSM), Acquity™ 4-position heated column manager, 2777 Ultra High Pressure Autosampler and a Xevo-TQ MS Triple Quadrupole mass spectrometer (Waters Ltd, Herts, UK). 1-Hydroxymidazolam was resolved on an Acquity™ HSS T3 (1.8 µm) column (2.1 x 30 mm; Waters Ltd) at 40 °C with a gradient of methanol (0-95-95%, 0-0.6-0.65 min) in 0.1% (v/v) aqueous formic acid containing 10 mM ammonium formate. The flow rate was 1 mL/min. Nitrogen was used as the nebulizing gas. The source temperature was 150 °C, the desolvation temperature was 650 °C, and the cone voltage and collision energy was 35 V and 30 eV, respectively. Data were processed with TargetLynx XS MassLynx 4.1 software (Waters Ltd). Consistent with published literature (Zimmerlin et al., 2011), formation of 1-hydroxymidazolam in the assays was monitored by peak area response. This gave acceptable dynamic detection ranges, determined by mean analyte signal-to-noise ratio above background MS response in the presence of maximal inhibition with the positive control inhibitor compared to the uninhibited (vehicle control) condition, corresponding to 674 to 6364 (for 0.75 µM

Downloaded from dmd.aspetjournals.org at ASPET Journals on November 15, 2019

DMD Fast Forward. Published on October 22, 2018 as DOI: 10.1124/dmd.118.083832
This article has not been copyedited and formatted. The final version may differ from this version.

midazolam incubations) and 3561 to 15357 (for 15 µM midazolam incubations) for reversible inhibition experiments, or 290 to 2841 for time-dependent inhibition experiments.

Mechanistic static prediction of simvastatin acid AUC change for the known clinical DDI perpetrated by telithromycin based upon determined in vitro OATP1B1 and CYP3A4 inhibitory parameters

The mean OATP1B1 IC_{50} (equating to K_i) and CYP3A4 K_i and K_I / k_{inact} values obtained for telithromycin were incorporated into the adapted Rowland-Matin mechanistic static equation previously described by Elsby et al. (2012, 2016) for reversible inhibition (Equation 1), but which has subsequently been modified to include a time-dependent inhibition component for CYP enzymes (Equation 3), in order to predict the change in simvastatin acid AUC based upon inhibition of an OATP1B1 fraction excreted (f_e) value of 0.79, and fraction metabolised (f_m) values of 0.40 and 0.83 for intestinal and hepatic CYP3A4, respectively (Elsby et al., 2012):

Equation 1 (reversible inhibition):

$$\mathrm{AUCR} = \frac{1}{\frac{f_{m/e}}{(1 + [I]/K_i)} + \left(1 - f_{m/e}\right)}$$

where K_i = absolute inhibition constant (equating to IC_{50} for transporters if the probe [S] <<<< K_m in the transporter inhibition assay and assuming competitive inhibition, based on the Cheng-Prusoff equation; Cheng et al. [1973]) and [I] = unbound maximum hepatic inlet concentration ($I_{in\ max\ u} = f_u \times (C_{max} + ((F_aF_g \times k_a \times \text{dose (mol)})/Q_h))/R_B$) for hepatic transporters/enzymes, or [I] = maximum enterocyte concentration ($I_g = (F_aF_g \times k_a \times \text{dose (mol)})/Q_{ent}$) for intestinal transporters/enzymes (Elsby et al., 2016). f_u = unbound fraction in plasma, C_{max} = maximum total plasma concentration of inhibitor at steady state, F_aF_g =

Downloaded from dmd.aspetjournals.org at ASPET Journals on November 15, 2019

DMD Fast Forward. Published on October 22, 2018 as DOI: 10.1124/dmd.118.083832
This article has not been copyedited and formatted. The final version may differ from this version.

fraction of the dose absorbed after oral administration, k_a = absorption rate constant (min^{-1}), Q_h = hepatic blood flow (1500 mL/min), R_B is the blood-to-plasma concentration ratio (default = 1.0) and Q_{ent} = enterocyte blood flow (300 mL/min).

Equation 2 (time-dependent inhibition R_2-value):

$$R_2 = \frac{k_{obs} + k_{deg}}{k_{deg}}$$

$$k_{obs} = \frac{k_{inact} \times [I]}{K_I + [I]}$$

$$R_2 = \frac{\frac{k_{inact} \times [I]}{K_I + [I]} + k_{deg}}{k_{deg}}$$

Equation 3 (reversible and time-dependent enzyme inhibition):

$$AUCR = \frac{1}{\frac{f_m}{(1 + [I]/K_i) \times \left[\frac{\frac{k_{inact} \times [I]}{K_I + [I]} + k_{deg}}{k_{deg}}\right]} + (1 - f_m)}$$

where k_{obs} = observed (apparent first order) inactivation rate constant of the affected enzyme, k_{deg} = apparent first-order degradation constant of the affected enzyme [for intestinal CYP3A4 = 0.00048 min^{-1} (Fahmi et al., 2009); hepatic CYP3A4 = 0.00032 min^{-1} (Obach et al., 2007)], k_{inact} = maximal inactivation rate constant, and K_I = inhibitor concentration causing half-maximal inactivation.

Downloaded from dmd.aspetjournals.org at ASPET Journals on November 15, 2019

DMD Fast Forward. Published on October 22, 2018 as DOI: 10.1124/dmd.118.083832
This article has not been copyedited and formatted. The final version may differ from this version.

RESULTS

Assessment of telithromycin as an inhibitor of OATP1B1 in vitro

Telithromycin demonstrated reproducible inter-assay concentration-dependent inhibition of OATP1B1-mediated transport of [^{3}H]-estradiol 17β-D-glucuronide (0.02 μM) with a mean (±S.D.) IC_{50} value of 12.0 ±1.45 μM (Table 1 and Fig. 1). Assessment of DDI potential via inhibition of hepatic OATP1B1 using the current FDA (2017) static equation approach gave an $R = 1 + [I_{in\ max\ u}]/K_i$ value of 1.21 (>1.1), indicating the potential for interaction in vivo (see Table 3 for [I] value). The positive control inhibitor, rifamycin SV (100 μM) gave acceptable inhibition (mean 95.1%) in the test system.

Assessment of telithromycin as a reversible or time dependent inhibitor of CYP3A4 in vitro (IC_{50} shift)

CYP3A4-mediated metabolism of midazolam (2.5 μM ≡ K_m) was inhibited by telithromycin in a concentration-dependent manner with IC_{50} values of 9.32 μM, 10.4 μM or 3.68 μM following a zero minute pre-incubation, a 30 min pre-incubation in the absence of NADPH, or a 30 min pre-incubation in the presence of NADPH, respectively. The 2.83-fold shift (decrease) in IC_{50} value following metabolic pre-incubation confirmed that telithromycin was both a reversible and time-dependent inhibitor of CYP3A4.

The positive control inhibitor mifepristone inhibited with IC_{50} values of 6.66 μM and 6.12 μM or 0.898 μM without (zero minute or minus NADPH), or with a metabolic pre-incubation, respectively. The 6.81-fold shift in IC_{50} value confirmed that the in vitro test system was able to detect both reversible and time-dependent inhibitors of CYP3A4.

Assessment of telithromycin as a reversible inhibitor of CYP3A4 in vitro (K_i determination)

Downloaded from dmd.aspetjournals.org at ASPET Journals on November 15, 2019

DMD Fast Forward. Published on October 22, 2018 as DOI: 10.1124/dmd.118.083832
This article has not been copyedited and formatted. The final version may differ from this version.

Telithromycin demonstrated reproducible inter-assay concentration-dependent inhibition of midazolam 1-hydroxylation in pooled human liver microsomes of a type that was determined to be of a competitive inhibitory nature with a mean (±S.D.) K_i of 3.65 ± 0.531 µM (Table 1 and Fig. 2), based on the rank ordering of type of inhibition by goodness of fit criteria as described above and shown in Table 2. Due to the low microsomal protein concentration used in the assay, microsomal binding in the test system was considered to be negligible. Assessment of DDI potential via reversible inhibition of intestinal or hepatic CYP3A4 using the current FDA (2017) static equation approach gave $R_{1,gut} = 1+[I_{gut}]/K_i$ or $R_1 = 1+[I_{max\ u}]/K_i$ values of 1081 (>11) or 1.26 (>1.02), respectively, indicating the potential for interaction in vivo (see Table 3 for [I] values). The positive control inhibitor ketoconazole fitted within acceptance criteria with a determined mean (±S.D.) K_i of 0.0248 ±0.00254 µM, using a non-competitive inhibition model.

Inactivation of CYP3A4 by telithromycin (K_I and k_{inact} determinations)

Telithromycin demonstrated both reproducible inter-assay time- and concentration-dependent inactivation of CYP3A4 activity (Table 1 and Fig. 3) with a determined mean (±S.D.) k_{inact} value of 0.02772 ±0.00272 min^{-1}, a mean (±S.D.) K_I value of 1.05 ± 0.226 µM and a mean (±S.D.) k_{inact}/K_I ratio of 28 ± 9.4 mL/min/µmol. Due to the low microsomal protein concentration used in the assay, microsomal binding in the test system was considered to be negligible. Assessment of DDI potential via time-dependent inhibition (inactivation) of hepatic CYP3A4 using the FDA (2012) static equation approach gave an $R_2 = (k_{obs} + k_{deg})/k_{deg}$ value of 64 (>1.25), indicating the potential for interaction in vivo (see Table 3 for [I] and k_{deg} values). The positive control inhibitor mifepristone fitted within acceptance criteria with determined mean (±S.D.) k_{inact}, K_I and k_{inact}/K_I ratio values of 0.07832 ±0.00553 min^{-1}, 0.865 ±0.166 µM and 92 ±11 mL/min/µmol, respectively.

Downloaded from dmd.aspetjournals.org at ASPET Journals on November 15, 2019

DMD Fast Forward. Published on October 22, 2018 as DOI: 10.1124/dmd.118.083832
This article has not been copyedited and formatted. The final version may differ from this version.

Predicted versus observed simvastatin acid AUC changes with telithromycin based upon in vitro OATP1B1 and CYP3A4 inhibitory data

Using the mean drug inhibitory affinities determined above for telithromycin versus OATP1B1 and CYP3A4 and its pharmacokinetic parameters provided in Table 3, calculations were performed with mechanistic static equations (1 and 3) in order to predict the theoretical fold-increase in simvastatin acid AUC that would occur following either their co-administration or being administered 12 hours apart.

Upon co-administration, the calculated predicted theoretical fold increases in AUC due to inhibition of hepatic OATP1B1, reversible inhibition of intestinal CYP3A4 and reversible inhibition of hepatic CYP3A4 were 1.16, 1.52 and 1.52-fold, respectively; collectively giving an overall AUCR of only 2.68. In contrast, calculated theoretical AUC increases due to time-dependent inactivation of intestinal or hepatic CYP3A4 alone were either 1.65-fold or 5.45-fold, respectively; maximum theoretical increases being 1.67-fold or 5.88-fold if each single pathway was completely ablated in DDI. Finally, the overall predicted AUC increase due to inhibition of OATP1B1 (1.16), combined reversible inhibition and inactivation of intestinal CYP3A4 (1.66) and combined reversible inhibition and inactivation of hepatic CYP3A4 (5.62) was 10.8-fold, which matched the clinically observed AUCR for simvastatin acid when co-administered with telithromycin (Table 4).

Upon dose staggering, using 12 h plasma unbound concentrations of telithromycin, the calculated predicted theoretical fold increases in AUC due to inhibition of hepatic OATP1B1, reversible inhibition of intestinal CYP3A4 and reversible inhibition of hepatic CYP3A4, were only 1.01, 1.01 and 1.02-fold, respectively. However, the overall predicted AUC increase due to inactivation of intestinal (1.49-fold) and hepatic (3.60-fold) CYP3A4 was 5.4-fold, which was within 33 % of the clinically observed AUCR for simvastatin acid when administered 12 hours apart from telithromycin (Table 4).

Downloaded from dmd.aspetjournals.org at ASPET Journals on November 15, 2019

DMD Fast Forward. Published on October 22, 2018 as DOI: 10.1124/dmd.118.083832
This article has not been copyedited and formatted. The final version may differ from this version.

DISCUSSION

DDIs with statins, in particular simvastatin (acid), are of clinical concern as elevated plasma concentrations of statins are linked to increased risk of myopathy (Egan and Coleman, 2011). As statins are common comedications across disease indications it is beneficial to project teams to be able to quantify, using mechanistic static models, the predicted DDI an investigational drug might perpetrate with these victim drugs in order to contextualise the clinical risk (Elsby et al., 2012; Williamson and Riley, 2017). However, pivotal to such accurate prediction is that the model incorporates all mechanisms of inhibition for metabolic enzymes to avoid underprediction of the clinical situation. One such underprediction of simvastatin acid AUCR, based on inhibition of CYP3A4 in the model, was reported previously for the DDI with telithromycin (Elsby et al., 2012). To reconcile this difference between prediction and the clinic, telithromycin was investigated in this study as a reversible and time-dependent inhibitor of CYP3A4 in vitro, alongside inhibition determined versus OATP1B1. The resulting inhibitory parameters were input into the mechanistic static model, newly modified to incorporate a time-dependent inhibition component for CYP, to ensure that the model now described complete enzyme inhibition potential in order to reproduce the clinically observed DDI with telithromycin, thereby ensuring the model's provision of more accurate prediction during future routine application with new drugs.

For simvastatin acid, active uptake (86%) into liver is mediated by the critical OATP1B1 pathway (Elsby et al., 2012). In the present study, the determined mean OATP1B1 IC_{50} for telithromycin versus estradiol 17β-D-glucuronide is approximately 10-fold more potent than previously reported versus sulfobromophthalein (Seithel et al., 2007), which was used in the earlier prediction (Elsby et al., 2012). This value is likely to be the most relevant as it has been derived 1) using a probe demonstrated to be a good OATP1B1 surrogate probe substrate for statins (Sharma et al., 2012; Izumi et al., 2015), and

Downloaded from dmd.aspetjournals.org at ASPET Journals on November 15, 2019

DMD Fast Forward. Published on October 22, 2018 as DOI: 10.1124/dmd.118.083832
This article has not been copyedited and formatted. The final version may differ from this version.

2) following a 15-min pre-incubation step with inhibitor to take into account any time-dependency required for the in vitro test system. For this determined IC_{50} value, even though the R-value is greater than the current FDA guidance cut-off (1.1), it is less than 1.25 which would be considered bioequivalent, suggesting that any interaction via inhibition of OATP1B1 in vivo is likely to have minimal effect. Indeed taking into account the OATP1B1 f_e, mechanistic static modelling predicted a minimal 1.16-fold increase in AUCR due to telithromycin co-administration, effectively confirming that inhibition of OATP1B1 would not be significant enough to impact simvastatin acid entry into hepatocytes nor its availability at CYP3A4 (i.e. no impact on f_m value).

The remaining critical disposition pathways of simvastatin acid include metabolism by intestinal and hepatic CYP3A4 (Elsby et al., 2012). Equivalent IC_{50} values determined from both the zero minute pre-incubation and the 30-min pre-incubation in the absence of NADPH confirmed telithromycin as a reversible inhibitor of CYP3A4 using the sensitive clinical probe midazolam. The reversible IC_{50} obtained in the shift assay was comparable to the 15 µM reported previously in recombinant CYP3A4 microsomes (Yoshida et al., 2012). According to the ordering of inhibition type by goodness of fit criteria, reversible inhibition type was determined to be competitive, which is supported by the fact that the determined K_i was about half the IC_{50} obtained from incubations using midazolam at a concentration equivalent to its K_m (Cheng and Prusoff, 1973). The in vitro test system was able to define correctly the mechanism of inhibition as demonstrated by the results for the positive control ketoconazole whose inhibitor type and mean K_i was consistent with literature data (Gibbs et al. 1999). Based on reversible CYP3A4 inhibition and determined R_1 values, telithromycin has the potential to cause a DDI via intestinal and hepatic CYP3A4 perturbation, thereby increasing the bioavailability of CYP3A4 substrate drugs by reducing their first-pass metabolism.

Downloaded from dmd.aspetjournals.org at ASPET Journals on November 15, 2019

DMD Fast Forward. Published on October 22, 2018 as DOI: 10.1124/dmd.118.083832
This article has not been copyedited and formatted. The final version may differ from this version.

Further to this, the IC_{50} shift assay also revealed telithromycin to be a time-dependent inhibitor of CYP3A4 based on the 2.83-fold decrease in IC_{50} following metabolic pre-incubation. The in vitro test system was suitable for such assessment as confirmed by the large shift observed for the positive control mifepristone and its determined mean K_I and k_{inact} values, which were consistent with literature data (He et al., 1999). Whilst, the ratio of k_{inact}/K_I for inactivation of CYP3A4 by telithromycin was approximately three times lower than the in vitro inactivation potency of mifepristone, the basic R_2 equation ratio (64) indicated a large potential for interaction in vivo based on this mechanism for telithromycin. To our knowledge this is the first reported in vitro study to demonstrate that telithromycin is a time-dependent inhibitor of CYP3A4.

Using mechanistic modelling, the predicted overall simvastatin acid AUCR (2.68) due to reversible inhibition of intestinal/hepatic CYP3A4 and inhibition of OATP1B1 in this study was lower than previously reported (4.0; Elsby et al., 2012). Reasons for this include: differences between F_aF_g and k_a parameters in the current analysis (that uses telithromycin-specific parameters 0.57 and 0.012) compared with the original analysis (that used default conservative values of 1.0 and 0.1, giving a 10x higher $I_{in\ max\ u}$); the use of enterocyte concentration (I_g) and f_m for intestinal CYP3A4 (based on Elsby et al., 2016) in this analysis, rather than the previous assumption of complete intestinal inhibition, and therefore maximal absorption, when intestinal luminal concentration/K_i>10 (Elsby et al., 2012). The absolute bioavailability value for telithromycin is considered to be equivalent to F_aF_g based on investigations in rat which established that high first pass metabolism of telithromycin is intestinal-mediated and not due to hepatic extraction (Lee and Lee, 2007). The use of such drug-specific parameters is favoured as it enables better predictability. Whilst reversible inhibition of intestinal CYP3A4 is predicted to almost completely inhibit that pathway following co-administration with telithromycin, the impact of hepatic inhibition is only

Downloaded from dmd.aspetjournals.org at ASPET Journals on November 15, 2019

DMD Fast Forward. Published on October 22, 2018 as DOI: 10.1124/dmd.118.083832
This article has not been copyedited and formatted. The final version may differ from this version.

predicted to be marginal (1.52-fold; 52% AUC increase compared with a theoretical maximum 488%, representing only approximately 10% of total activity). In contrast, reversible inhibition of intestinal/hepatic CYP3A4 (and of OATP1B1) is predicted to be negligible when the drugs are administered 12 h apart due to minimal telithromycin systemic plasma concentrations.

This analysis indicates time-dependent inhibition of CYP3A4 by telithromycin as the primary driver of observed DDIs with simvastatin acid. In order to confirm this the previous mechanistic static model (Elsby et al., 2012 & 2016) was modified to incorporate an enzyme inactivation component capturing parameters k_{inact}, K_I and k_{deg} for intestinal or hepatic CYP3A4, as detailed in Equation 3. Using this modified model it is clear that telithromycin-mediated inactivation of intestinal and hepatic CYP3A4 alone results in almost complete ablation of these simvastatin acid disposition pathways based on predictions of AUCR following their co-administration, when compared with theoretical AUCR maxim for each single pathway. Moreover, when the major effect of CYP3A4 inactivation is combined with the modest effect of reversible CYP3A4 inhibition and OATP1B1 inhibition, the overall predicted fold-increase in simvastatin acid AUC (10.8-fold) matched the clinically observed AUC increase (10.8-fold; 980% in study 1048, Ketek® FDA review 4). Additionally, the predicted AUCR following dose staggering was consistent with the clinical AUCR indicating CYP3A4 inactivation as the sole mechanism underlying that DDI.

The predictability of the model was evaluated further using drug-specific parameters for another perpetrator clarithromycin (500 mg), which is known to cause DDI with simvastatin acid resulting in a mean 11.6-fold increase in victim drug exposure (Ketek® FDA review 1; study 1067). Based on clarithromycin parameters (F_aF_g=0.89, k_a=0.0113 min^{-1}, f_u=0.30, CYP3A4 K_i=57.5 µM, K_I=13.2 µM, k_{inact}=0.058 min^{-1}, OATP1B1 K_i=5.3 µM and $C_{max\ ss}$=3.83 µM; Chu et al., 1992, Ikawa et al., 2014, Obach et al., 2006, Yoshida et al.,

Downloaded from dmd.aspetjournals.org at ASPET Journals on November 15, 2019

DMD Fast Forward. Published on October 22, 2018 as DOI: 10.1124/dmd.118.083832
This article has not been copyedited and formatted. The final version may differ from this version.

2012, Zimmerlin et al., 2011, Vermeer et al., 2016, Ketek® FDA review 1) yielding calculated [I_g] and [$I_{in\ max\ u}$] of 22.4 and 2.493 µM, predicted AUCRs due to inhibition of intestinal CYP3A4, OATP1B1 and hepatic CYP3A4 were 1.66, 1.34 and 5.08, respectively. The resulting predicted combined AUCR of 11.3 was similar to the clinically observed value. Interestingly, like telithromycin, the magnitude of DDI due to clarithromycin is primarily a consequence of time-dependent inhibition of CYP3A4. Correct predictions of simvastatin acid AUCR for DDIs mediated by telithromycin and clarithromycin validate the modified, integrated mechanistic static equation in the model. Moreover, the finding that for the DDIs above, predicted AUCR values calculated by the net-effect model (Fahmi et al., 2009; detailed in the FDA draft DDI guidance 2017) were identical to those values derived via Equation 3, verified the model (data not shown).

In conclusion, the modified mechanistic static equation (3) incorporating both reversible and time-dependent inhibition for CYP enzymes, which has been successfully applied in this study to understand the mechanism of DDI between simvastatin acid and telithromycin, will provide a useful tool for use in drug discovery and development towards quantitative prediction of more complex DDIs, which can subsequently inform decision-making and clinical protocol design for patient studies.

Downloaded from dmd.aspetjournals.org at ASPET Journals on November 15, 2019

DMD Fast Forward. Published on October 22, 2018 as DOI: 10.1124/dmd.118.083832
This article has not been copyedited and formatted. The final version may differ from this version.

ACKNOWLEDGEMENTS

We would like to acknowledge Chris Turner, Andrew Blainey and Roisin Toohey for conducting some of the in vitro enzyme experiments.

Downloaded from dmd.aspetjournals.org at ASPET Journals on November 15, 2019

DMD Fast Forward. Published on October 22, 2018 as DOI: 10.1124/dmd.118.083832
This article has not been copyedited and formatted. The final version may differ from this version.

AUTHORSHIP CONTRIBUTIONS

Participated in research design: Elsby, Plant

Conducted experiments: Hare, Neal, Outteridge, Pearson, Upcott Gill

Performed data analysis: Elsby, Hare, Neal, Outteridge, Pearson, Upcott Gill

Wrote or contributed to the writing of the manuscript: Butler, Elsby, Hare, Neal, Outteridge, Pearson, Plant, Riley, Upcott Gill

Downloaded from dmd.aspetjournals.org at ASPET Journals on November 15, 2019

DMD Fast Forward. Published on October 22, 2018 as DOI: 10.1124/dmd.118.083832
This article has not been copyedited and formatted. The final version may differ from this version.

REFERENCES

Cheng Y and Prusoff WH (1973) Relationship between the inhibition constant (K_i) and the concentration of inhibitor which causes 50 per cent inhibition (I_{50}) of an enzymatic reaction. *Biochem Pharmacol* **22:** 3099-3108.

Chu SY, Deaton R and Cavanaugh J (1992) Absolute bioavailability of clarithromycin after oral administration in humans. *Antimicrob Agents Chemother* **36:** 1147-1150.

Egan A and Colman E (2011) Weighing the benefits of high-dose simvastatin against the risk of myopathy. *N Engl J Med* **365:** 285–287.

Elsby R, Hilgendorf C and Fenner K (2012) Understanding the critical disposition pathways of statins to assess drug-drug interaction risk during drug development: it's not just about OATP1B1. *Clin Pharmacol Ther* **92:** 584-598.

Elsby R, Martin PD, Surry D, Sharma P and Fenner K (2016) Solitary inhibition of the breast cancer resistance protein (BCRP) efflux transporter results in a clinically significant drug-drug interaction with rosuvastatin by causing up to a two-fold increase in statin exposure. *Drug Metab Dispos* **44:** 398-408.

Fahmi OA, Hurst S, Plowchalk D, Cook J, Guo F, Youdim K, Dickins M, Phipps A, Darekar A, Hyland R and Obach RS (2009) Comparison of different algorithms for predicting clinical drug-drug interactions, based on the use of CYP3A4 in vitro data: predictions of compounds as precipitants of interaction. *Drug Metab Dispos* **37:** 1658-1666.

Downloaded from dmd.aspetjournals.org at ASPET Journals on November 15, 2019

DMD Fast Forward. Published on October 22, 2018 as DOI: 10.1124/dmd.118.083832
This article has not been copyedited and formatted. The final version may differ from this version.

Gibbs MA, Thummel KE, Shen DD and Kunze KL (1999) Inhibition of cytochrome P-450 3A (CYP3A) in human intestinal and liver microsomes: comparison of K_I values and impact of CYP3A5 expression. *Drug Metab Dispos* **27:** 180-187.

He K, Woolf TF and Hollenberg PF (1999) Mechanism-based inactivation of cytochrome P-450-3A4 by mifepristone (RU486). *J Pharmacol Exp Ther* **288:** 791-797.

Ikawa K , Kikuchi E, Kikuchi J, Nishimura M, Derendorf H and Morikawa N (2014) Pharmacokinetic modelling of serum and bronchial concentrations for clarithromycin and telithromycin, and site-specific pharmacodynamic simulation for their dosages. *J Clin Pharm Ther* **39:** 411-417.

Izumi S, Nozaki Y, Maeda K, Komori T, Takenaka O, Kusuhara H and Sugiyama Y (2015) Investigation of the impact of substrate selection on in vitro organic anion transporting polypeptide 1B1 inhibition profiles for the prediction of drug-drug interactions. *Drug Metab Dispos* **43:** 235-247.

Ketek® (telithromycin) US FDA drug label (Ref ID 2874174), 2010; Sanofi-Aventis. Accessed via Drugs@FDA database (www.accessdata.fda.gov/scripts/cder/daf/) on 26 June 2018.

Ketek® (telithromycin) US FDA review 1 (Clinical Pharmacology and Biopharmaceutics Review Part 1; NDA number 21-144), 2003; Aventis Pharmaceuticals. Accessed via Drugs@FDA database (https://www.accessdata.fda.gov/drugsatfda_docs/nda/2004/21-144_Ketek.cfm) on 26 June 2018.

Downloaded from dmd.aspetjournals.org at ASPET Journals on November 15, 2019

DMD Fast Forward. Published on October 22, 2018 as DOI: 10.1124/dmd.118.083832
This article has not been copyedited and formatted. The final version may differ from this version.

Ketek® (telithromycin) US FDA review 4 (Clinical Pharmacology and Biopharmaceutics Review Part 4; NDA number 21-144), 2003; Aventis Pharmaceuticals. Accessed via Drugs@FDA database (https://www.accessdata.fda.gov/drugsatfda_docs/nda/2004/21-144_Ketek.cfm) on 26 June 2018.

Lee JH and Lee MG (2007) Dose-dependent pharmacokinetics of telithromycin after intravenous and oral administration to rats: contribution of intestinal first-pass effect to low bioavailability. *J Pharm Pharm Sci* **10:** 37-50.

Obach RS, Walsky RL, Venkatakrishnan K, Gaman EA, Houston JB and Tremaine LM (2006) The utility of in vitro cytochrome P450 inhibition data in the prediction of drug-drug interactions. *J Pharmacol Exp Ther* **316:** 336-348.

Obach RS, Walsky RL and Venkatakrishnan K (2007) Mechanism-based inactivation of human cytochrome p450 enzymes and the prediction of drug-drug interactions. *Drug Metab Dispos* **35:** 246-255.

Seithel A, Eberl S, Singer K, Auge D, Heinkele G, Wolf NB, Dörje F, Fromm MF and König J (2007) The influence of macrolide antibiotics on the uptake of organic anions and drugs mediated by OATP1B1 and OATP1B3. *Drug Metab Dispos* **35:** 779-786.

Sharma P, Butters CJ, Smith V, Elsby R and Surry D (2012) Prediction of the in vivo OATP1B1-mediated drug-drug interaction potential of an investigational drug against a range of statins. *Eur J Pharm Sci* **47:** 244-255.

Downloaded from dmd.aspetjournals.org at ASPET Journals on November 15, 2019

DMD Fast Forward. Published on October 22, 2018 as DOI: 10.1124/dmd.118.083832
This article has not been copyedited and formatted. The final version may differ from this version.

US Food and Drug Administration. (2012). Draft guidance for industry: Drug interaction studies – study design, data analysis, implications for dosing, and labelling recommendations (available at http://www.fda.gov/downloads/Drugs/GuidanceComplianceRegulatoryInformation/Guidances/UCM292362.pdf; accessed 01 December 2014).

US Food and Drug Administration. (2017). Draft guidance for industry: In vitro metabolism- and transporter-mediated drug-drug interaction studies (available at http://www.fda.gov/downloads/Drugs/GuidanceComplianceRegulatoryInformation/Guidances/UCM581965.pdf; accessed 26 October 2017).

Vermeer LM, Isringhausen CD, Ogilvie BW and Buckley DB (2016) Evaluation of ketoconazole and its alternative clinical CYP3A4/5 inhibitors as inhibitors of drug transporters: the in vitro effects of ketoconazole, ritonavir, clarithromycin, and itraconazole on 13 clinically-relevant drug transporters. *Drug Metab Dispos* **44:** 453-459.

Vieira ML, Zhao P, Berglund EG, Reynolds KS, Zhang L, Lesko LJ and Huang SM (2012) Predicting drug interaction potential with a physiologically based pharmacokinetic model: a case study of telithromycin, a time-dependent CYP3A inhibitor. *Clin Pharmacol Ther* **91:** 700-708.

Williamson B and Riley R (2017) Hepatic transporter drug-drug interactions: an evaluation of approaches and methodologies. *Expert Opin drug Metab Toxicol* **13:** 1237-1250.

Downloaded from dmd.aspetjournals.org at ASPET Journals on November 15, 2019

DMD Fast Forward. Published on October 22, 2018 as DOI: 10.1124/dmd.118.083832
This article has not been copyedited and formatted. The final version may differ from this version.

Yoshida K, Maeda K and Sugiyama Y (2012) Transporter-mediated drug-drug interactions involving OATP substrates: predictions based on in vitro inhibition studies. *Clin Pharmacol Ther* **91:** 1053-1064.

Zimmerlin A, Trunzer M and Faller B (2011) CYP3A time-dependent inhibition risk assessment validated with 400 reference drugs. *Drug Metab Dispos* **39:** 1039-1046.

Zocor® (simvastatin) US FDA drug label (Ref ID 3087218), February 2012; Merck Sharp & Dohme. Accessed via Drugs@FDA database (www.accessdata.fda.gov/scripts/cder/daf/) on 25 July 2018.

Downloaded from dmd.aspetjournals.org at ASPET Journals on November 15, 2019

DMD Fast Forward. Published on October 22, 2018 as DOI: 10.1124/dmd.118.083832
This article has not been copyedited and formatted. The final version may differ from this version.

FOOTNOTES

None.

Downloaded from dmd.aspetjournals.org at ASPET Journals on November 15, 2019

DMD Fast Forward. Published on October 22, 2018 as DOI: 10.1124/dmd.118.083832
This article has not been copyedited and formatted. The final version may differ from this version.

LEGENDS FOR FIGURES

Fig. 1. Representative plot of mean concentration-dependent inhibition of OATP1B1-mediated transport of [^{3}H]-estradiol 17β-D-glucuronide (0.02 μM) by telithromycin. Data are expressed as mean (± standard deviation) from triplicate wells per incubation condition.

Fig. 2. Representative Michaelis-Menten plot (competitive inhibition) (A), Eadie-Hofstee plot (competitive inhibition) (B) and Dixon plot (competitive inhibition) (C) of the effect of telithromycin on CYP3A4-mediated 1-hydroxymidazolam formation in pooled human liver microsomes. Data are expressed as mean (± standard error) from duplicate wells. [I] = telithromycin concentration (nM), [S] = midazolam concentration (nM).

Fig. 3. Representative plot of natural logarithm of the corrected percentage CYP3A4 activity remaining against pre-incubation time based on the effect of telithromycin on 1-hydroxymidazolam formation in pooled human liver microsomes (A). Non-linear (Michaelis-Menten) regression plot of the observed rates of enzyme inactivation against inhibitor concentration for telithromycin (B). Data are expressed as mean from duplicate wells.

Downloaded from dmd.aspetjournals.org at ASPET Journals on November 15, 2019

Downloaded from dmd.aspetjournals.org at ASPET Journals on November 15, 2019

TABLES

Table 1: Determined in vitro inhibitory kinetic parameters of telithromycin versus OATP1B1 and CYP3A4

Type	Determined inhibitory kinetic parameter values						
	Expt 1	**Expt 2**	**Expt 3**	**Mean**	**S.D.**	**CV(%)**	**95% CI***
OATP1B1 K_i (IC_{50}) (μM)	13.7	11.3	11.1	12.0	1.45	12.1	8.40 – 15.6
CYP3A4 K_i (μM)	3.68	4.29	2.99	3.65	0.531	14.5	2.33 – 4.97
CYP3A4 K_I (μM)	1.15	0.786	1.20	1.05	0.226	21.5	0.489 – 1.61
CYP3A4 k_{inact} (min^{-1})	0.02492	0.03036	0.02790	0.02772	0.00272	9.8	0.02096 – 0.03448

K_i = absolute inhibition constant versus the enzyme or transporter (for OATP1B1; assuming competitive inhibition, this equates to IC_{50} in the assay as probe substrate concentration utilised is <<<< K_m)

K_I = inhibitor concentration causing half-maximal inactivation

k_{inact} = maximal rate of inactivation of the enzyme

*95% confidence interval was calculated by adding or subtracting the product of the t-distribution value (4.303) and the value of the standard deviation divided by the square root of the sample size from the determined mean value.

Downloaded from dmd.aspetjournals.org at ASPET Journals on November 15, 2019

Table 2. Determination of K_i and observed fit to different inhibition models for the inhibition of CYP3A4-mediated 1-hydroxylation of midazolam by telithromycin in pooled human liver microsomes.

Inhibition type	Rate equation	Experiment 1			Experiment 2			Experiment 3		
		K_i (μM)	R^2	AICc	K_i (μM)	R^2	AICc	K_i (μM)	R^2	AICc
Competitive	$v = \frac{Vmax\,[S]}{[S] + K_m\left(1+\frac{[I]}{K_i}\right)}$	3.68	0.989	-515	4.29	0.994	-563	2.99	0.988	-439
Non-competitive	$v = \frac{Vmax\,[S]}{K_m\left(1+\frac{[I]}{K_i}\right)+[S]\left(1+\frac{[I]}{K_i}\right)}$	16.9	0.974	-453	16.8	0.975	-458	14.1	0.968	-371
Uncompetitive	$v = \frac{Vmax\,[S]}{K_m+[S]\left(1+\frac{[I]}{K_i}\right)}$	11.0	0.945	-399	10.1	0.943	-400	9.07	0.935	-322
Mixed*	$v = \frac{Vmax\,[S]}{K_m\left(1+\frac{[I]}{K_i}\right)+[S]\left(1+\frac{[I]}{\alpha K_i}\right)}$	4.33	0.990	-516	4.29	0.994	-561	3.10	0.988	-437

*α value for mixed inhibition determined to be 26.9, 15.6, and 151 for experiments 1, 2 and 3, respectively

Downloaded from dmd.aspetjournals.org at ASPET Journals on November 15, 2019

R^2 = squared correlation coefficient

AICc = corrected Akaike's Information Criterion

v = rate of metabolite formation

V_{max} = maximal rate of metabolite formation

K_m = Michaelis-Menten constant

[S] = probe substrate concentration

K_i = absolute inhibition constant

Downloaded from dmd.aspetjournals.org at ASPET Journals on November 15, 2019

Table 3: Pharmacokinetic parameters of telithromycin in clinical interaction studies with simvastatin acid.

Perpetrator drug	**Dose (mg)**	**MW**	**[I_g] (μM)**	**[C_{max}] or [C_{12h}] (μM)**	**f_u**	**[$C_{12h\ u}$] (μM)**	**[$I_{in\ max}$] (μM)**	**[$I_{in\ max\ u}$] (μM)**
Telithromycin (co-admin)	800	812	22.5	2.76	0.35	NA	7.25	2.538
Telithromycin (12h apart)	800	812	NA	0.246	0.35	0.086	NA	NA

f_u = median fraction unbound (taken from the Ketek® drug label accessed via Drugs@FDA database; https://www.accessdata.fda.gov/scripts/cder/daf))

NA = Not applicable to DDI

[I_g] = maximal enterocyte concentration and [$I_{in\ max}$] = maximum hepatic inlet concentration; calculated as described in Materials and Methods using telithromycin-specific values of F_aF_g = 0.57 (FDA drug label) and k_a = 0.012 min^{-1} (0.740 h^{-1}) (Ikawa et al., 2014)

[C_{max}] = Mean steady-state maximum plasma concentration for total (bound plus unbound) drug measured in the clinical interaction study with simvastatin acid (Study Number 1048; Ketek® FDA approval package review 4 (Clinical Pharmacology Biopharmaceutics Review Part 4, accessed via Drugs@FDA database; https://www.accessdata.fda.gov/drugsatfda_docs/nda/2004/21-144_Ketek.cfm))

Downloaded from dmd.aspetjournals.org at ASPET Journals on November 15, 2019

$[C_{12h}]$ = Plasma concentration for total (bound plus unbound) drug at T=12 h (0.2 mg/L) measured in the clinical interaction study with simvastatin acid (Study Number 1048, HMR3647 AUC profile; Ketek® FDA approval package review 4)

Downloaded from dmd.aspetjournals.org at ASPET Journals on November 15, 2019

Table 4: Predicted versus observed AUC increases of simvastatin acid following co-administration or dose staggering (12 h apart) with telithromycin based upon combined reversible inhibition/inactivation of intestinal CYP3A4 (f_m = 0.4) and hepatic CYP3A4 (f_m = 0.83) with inhibition of hepatic OATP1B1 (f_e = 0.79).

Perpetrator drug	Dose (mg)	Predicted fold increase in AUC due to inhibition of composite pathways			Overall predicted AUCR	Clinically observed AUCR	Primary mechanism of DDI
		Intestinal CYP3A4 *(theoretical max = 1.67)*	OATP1B1 *(theoretical max = 4.76)*	Hepatic CYP3A4 *(theoretical max = 5.88)*			
Telithromycin (co-admin)	800	1.66 [1.66 – 1.67]	1.16 [1.12 – 1.22]	5.62 [5.45 – 5.74]	10.8 [10.1 – 11.7]	9.4[a]-10.8[b]	CYP3A4 reversible inhibition/inactivation
Telithromycin (12h apart)	800	1.49# [1.38 – 1.58]	1.01# [1.00 - 1.01]	3.60# [2.79 – 4.62]	5.4 [3.85 – 7.37]	4.3[a]	CYP3A4 inactivation

[a] Study Number 1065; Drug FDA approval package review 1 (Clinical Pharmacology Biopharmaceutics Review Part 1, accessed via Drugs@FDA database; https://www.accessdata.fda.gov/drugsatfda_docs/nda/2004/21-144_Ketek.cfm)

[b] Study Number 1048; Drug FDA approval package review 4 (Clinical Pharmacology Biopharmaceutics Review Part 4, accessed via Drugs@FDA database; https://www.accessdata.fda.gov/drugsatfda_docs/nda/2004/21-144_Ketek.cfm)

Downloaded from dmd.aspetjournals.org at ASPET Journals on November 15, 2019

using [$C_{12h\ u}$] plasma concentration for [I]

[ ] numbers in square brackets are the calculated predicted AUCR range using the upper and lower 95% confidence intervals determined for each inhibitory kinetic parameter given in Table 1. To determine the lower predicted AUCR, the upper confidence interval for K_i and K_I values and the lower confidence interval for k_{inact} were used for calculations. To determine the upper predicted AUCR, the lower confidence interval for K_i and K_I values and the upper confidence interval for k_{inact} were used for calculations.

DMD Fast Forward. Published on October 22, 2018 as DOI: 10.1124/dmd.118.083832
This article has not been copyedited and formatted. The final version may differ from this version.

Figure 1

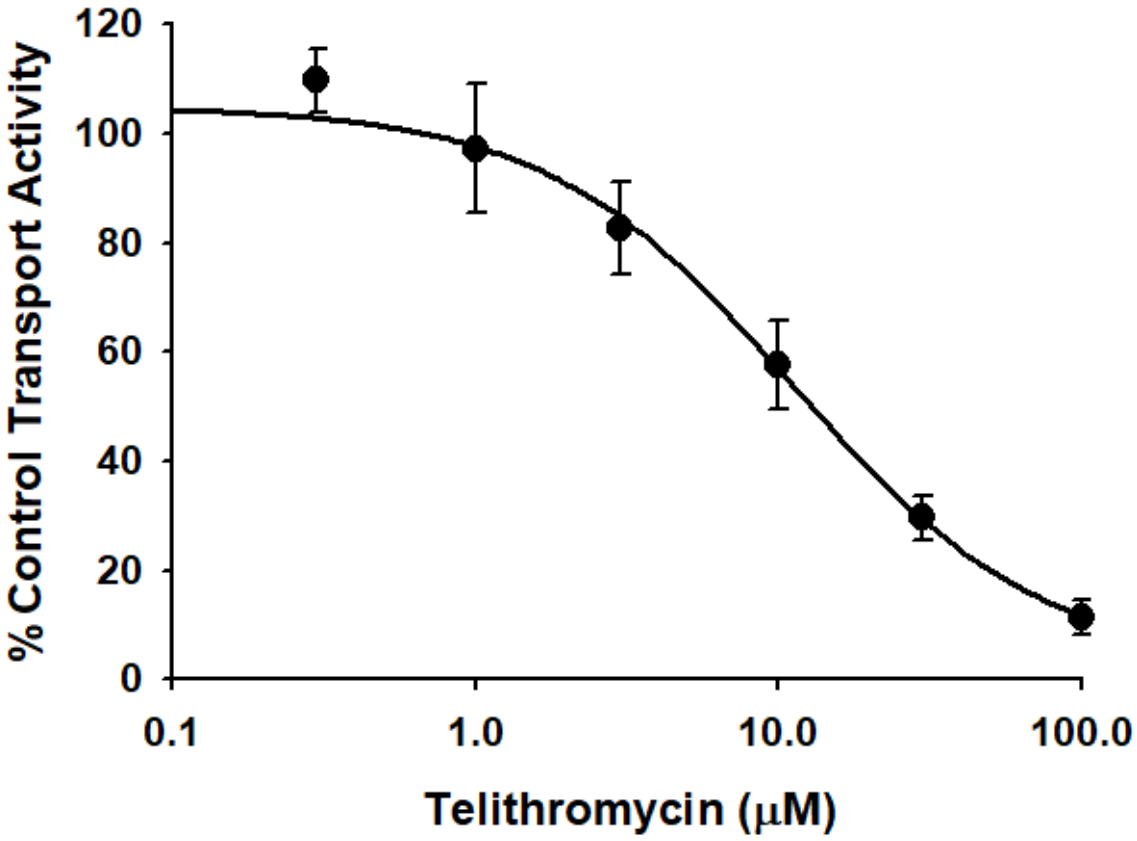

Downloaded from dmd.aspetjournals.org at ASPET Journals on November 15, 2019

DMD Fast Forward. Published on October 22, 2018 as DOI: 10.1124/dmd.118.083832
This article has not been copyedited and formatted. The final version may differ from this version.

Figure 2

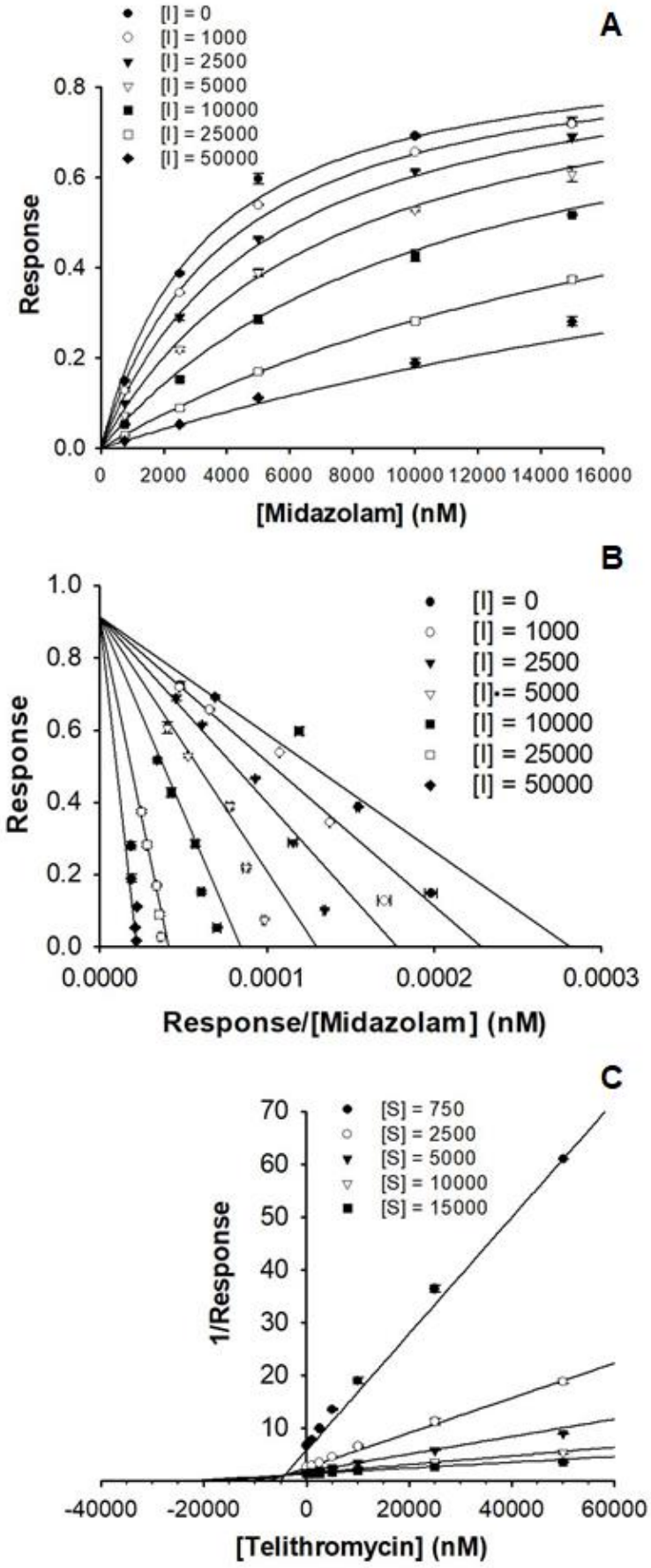

Downloaded from dmd.aspetjournals.org at ASPET Journals on November 15, 2019

Figure 3

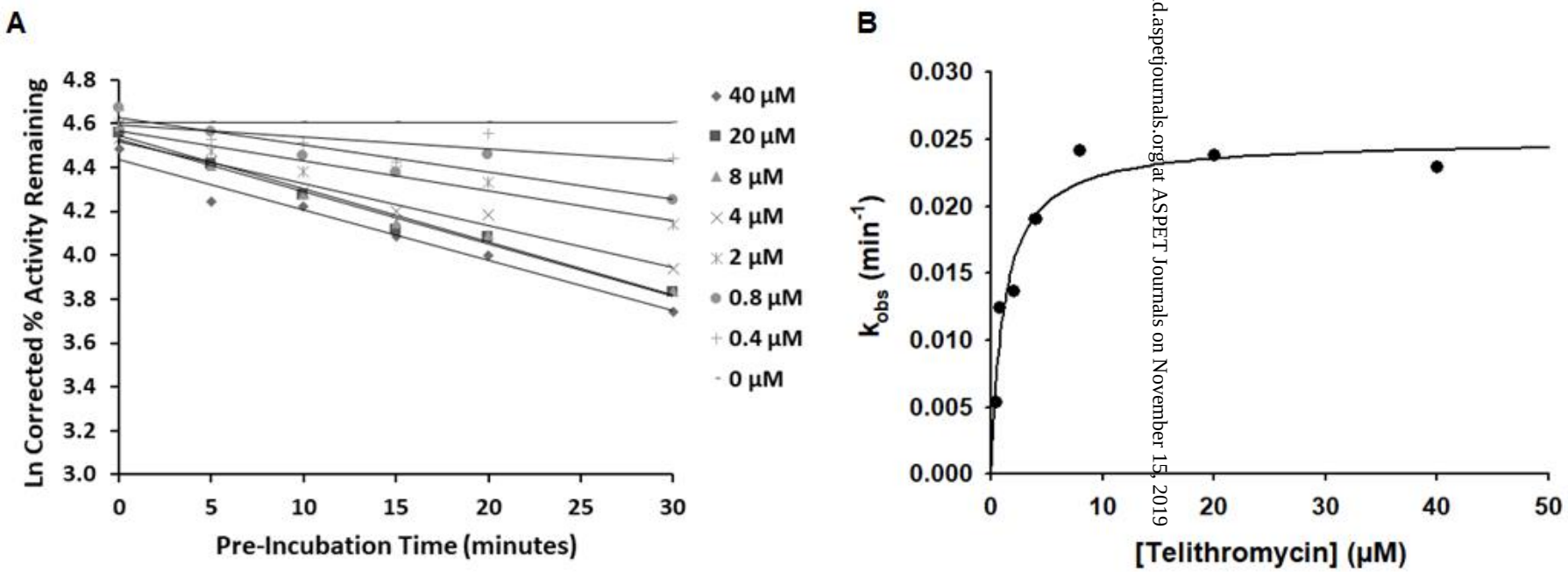

Downloaded from dmd.aspetjournals.org at ASPET Journals on November 15, 2019